Progress in Fractional Differentiation and Applications
An International Journal

http://dx.doi.org/10.18576/pfda/020401

Numerical Studies for the Fractional Schrödinger Equation with the Quantum Riesz-Feller Derivative

Nasser Hassan Sweilam and Muner Mustafa Abou Hasan*

Department of Mathematics, Faculty of Science, Cairo University, Giza, Egypt

Received: 15 Feb. 2016, Revised: 23 May 2016, Accepted: 25 May 2016
Published online: 1 Oct. 2016

Abstract: In this paper, we present a numerical method for solving the one-dimensional space fractional Schrödinger equation in the case of a particle moving in a potential field. The fractional derivative is defined by the quantum Riesz-Feller fractional derivative. A novel weighted average non-standard finite difference method is presented to solve the underline problem numerically. The stability analysis of the proposed method is given by a recently proposed procedure similar to the standard John von Neumann stability analysis and the truncation error is analyzed. Several numerical examples are introduced for various choices of derivative order $\alpha,\ 1<\alpha\leq 2$, and for various choices of skewness θ to demonstrate utility of the proposed method. We demonstrate that the proposed technique is more accurate than the standard weighted average finite difference method.

Keywords: Space fractional Schrödinger equation, Riesz-Feller fractional derivative, weighted average non-standard finite difference methods, von Neumann stability analysis.

1 Introduction

The famous Schrödinger equation is one of the fundamental equations in quantum mechanics that describes the change of the quantum behavior of some physical systems, It was formulated in 1925, by the Austrian physicist Erwin Schrödinger.

It was shown in [1] that the Feynman path integral over the Lévy like quantum-mechanical paths allows to develop a fractional generalization of the quantum mechanics. Whereas the Feynman path integral over Brownian trajectories leads to the well-known Schrödinger equation, the path integrals over Lévy trajectories lead to the fractional Schrödinger equation (FSE) with the quantum Riesz derivative. Nick Laskin [1] discovered the fundamental equation of FSE in the form:

$$i\hbar\frac{\partial\Psi(r,t)}{\partial t}=C_\alpha(m)(-\Delta)^{\alpha/2}\Psi(r,t)+V(r,t)\Psi(r,t),\quad t\geq 0,\quad r\in\mathbb{R}, \tag{1}$$

for the wave function Ψ of a quantum particle with the mass m that moves in a potential field with the potential V. In (1), $\hbar=\frac{h}{2\pi}$, where h is the Plank constant. $C_\alpha(m)$ is a positive constant which equals $\frac{\hbar^2}{2m}$ for $\alpha=2$ [2], and $(-\Delta)^{\alpha/2}$ was called in ([3], [1]) the quantum Riesz fractional derivative of order α. In the mathematical literature, $(-\Delta)^{\alpha/2}$ is usually referred to as the fractional Laplacian. For $\alpha=2$, the quantum Riesz fractional derivative becomes the negative Laplace operator $-\Delta$ and Eq. (1) is reduced to the classical Schrödinger equation for a quantum particle with the mass m that moves in a potential field with the potential V.

The non-standard finite difference (NSFD) schemes were firstly proposed by Mickens [4], both for ordinary differential equations (ODEs) and partial differential equations (PDEs) with more accuracy than standard finite difference method (SFDM), Recently Sweilam *et al.* ([5], [6]) used this technique to solve fractional and variable order fractional differential equations, also they used to solve Two-dimensional fractional diffusion equation [7].

The purpose of this work is to study numerically the fractional Schrödinger equation with the quantum Riesz-Feller derivative for a particle that moves in a potential field using new technique called weighted average non-standard finite difference method (WA-NSFDM) and to illustrate the behavior of the solutions of FSE with various values of α and θ.

* Corresponding author e-mail: nsweilam@sci.cu.edu.eg

Numerical results are given to highlight the high accuracy of the present method. Recently, in 2013, Al Saqabi [3] showed that this model with the quantum Riesz-Feller derivative can be considered from the mathematical viewpoint, but it seems to have no physical applications in the case $\theta \neq 0$.

Several analytical and numerical methods (see e.g. [8], [3], [1] to mention only few of them) have been proposed for the one-dimensional space-fractional and space-time-fractional Schrödinger equations with some specific potential fields including zero potential (free particle), the δ-potential, the infinite potential well, the Coulomb potential, and a rectangular barrier. In [9] the authors introduced the implicit fully discrete local discontinuous Galerkin method (IFDLDGM) for a solution of the T-FSE, while Mohebbi *et al.* [10] used the meshless technique (MT) for approximating its solution numerically. Moreover, Bhrawy *et al.* [11] proposed a new Jacobi spectral collocation method for solving fractional Schrödinger equations and fractional coupled Schrödinger system. More recently, Bhrawy *et al.* [12] proposed a fully spectral collocation approximation for multi-dimensional time fractional Schrödinger equations.

This paper is structured as follows: In the next section we give some definitions on fractional calculus and some properties of non-standard discretization. Section 3 is devoted to discretization of the Cauchy-type problem for fractional Schrödinger equation with the quantum Riesz-Feller derivative in the case of a free particle using weighted average non-standard finite difference methods. In Section 4 stability analysis and truncating error of the proposed method for solving the mention model were studied. In Section 5 some numerical treatments are establishment with their results. Concluding remarks are given in Section 6.

2 Preliminaries and Notations

This section gives some preliminary results which are needed in subsequent sections of this paper.

2.1 Fractional Calculus Definitions

In the last years fractional derivatives have found numerous applications in many fields of physics, mechanical engineering, biology, electrical engineering, control theory and finance ([13], [14], [15], [6], [4]). Fractional calculus in mathematics is a natural extension of integer-order calculus and gives a useful mathematical tool for modeling many processes in nature more than classic calculus.

Indeed, many definitions of the fractional integrals and derivatives were introduced (see e.g. [16]). The time-fractional derivatives are often given in the Caputo, Riemann-Liouville, or Grünwald-Letnikov sense. As to the space-fractional derivative, it is usually defined as an operator inverse to the Riesz potential (see e.g. [17], [14], [1]) and is referred to as the Riesz fractional derivative. Podlubny mentioned (in [18]) that "the complete theory of fractional differential equations, especially the theory of boundary value problems for fractional differential equations, can be developed only with the use of both left-and right-sided derivatives." So the spatial derivatives discussed in this paper are all Riesz-Feller potential operator, which include the two-sided Riemann-Liouville fractional derivatives. Recently, the Riesz-Feller space-fractional derivative of order α and skewness θ has been shown to be relevant for anomalous diffusion models [14]. In addition, this derivative is better suited for a generalization to higher order derivatives. Another advantage of using Riesz-Feller derivative lies in the fact that the solution of the fractional reaction-diffusion equation with Riesz-Feller derivative includes the fundamental solution for space-time reactional diffusion, which itself is a generalization of neutral fractional diffusion, space-fractional diffusion, and time-fractional diffusion [19].
For $0<\alpha<2$ and $|\theta| \leq min\{\alpha, 2-\alpha\}$, the quantum Riesz-Feller derivative can be represented in the form (see e.g. [3], [20], [16])

$$D^{\alpha}_{\theta} f(x) = -\frac{\Gamma(1+\alpha)}{\pi} \left\{ sin\left((\alpha+\theta)\frac{\pi}{2}\right) \int_0^{\infty} \frac{f(x+\xi)-f(x)}{\xi^{1+\alpha}} d\xi + sin\left((\alpha-\theta)\frac{\pi}{2}\right) \int_0^{\infty} \frac{f(x-\xi)-f(x)}{\xi^{1+\alpha}} d\xi \right\}. \tag{2}$$

For $0<\alpha<2$ and $\alpha \neq 1$ and θ in its range, this formula can be rewritten as (see e.g. [3], [14])

$$D^{\alpha}_{\theta} f(x) = (c_+ D^{\alpha}_{+} + c_- D^{\alpha}_{-}) f(x), \tag{3}$$

where the coefficients $c_{\pm}$ are given by

$$c_+ = c_+(\alpha,\theta) = \frac{sin((\alpha-\theta)\pi/2)}{sin(\alpha\pi)}, \quad c_- = c_-(\alpha,\theta) = \frac{sin((\alpha+\theta)\pi/2)}{sin(\alpha\pi)}, \tag{4}$$

and

$$(D_+^\alpha f)(x) = (\frac{d}{dx})^n (I_+^{n-\alpha} f)(x), \;\; (D_-^\alpha f)(x) = (-\frac{d}{dx})^n (I_-^{n-\alpha} f)(x), \tag{5}$$

are the two-sided Riemann-Liouville fractional derivatives with $x \in \mathbb{R}$ and $\alpha > 0,\; n-1 < \alpha \le n,\; n \in \mathbb{N}$. In expressions (5) the fractional operators $I_\pm^{n-\alpha}$ are defined as the left- and right-side of Weyl fractional integrals, which given by

$$(I_+^\alpha f)(x) = \frac{1}{\Gamma(\alpha)} \int_{-\infty}^{x} \frac{f(\xi)}{(x-\xi)^{1-\alpha}} d\xi, \;\; (I_-^\alpha f)(x) = \frac{1}{\Gamma(\alpha)} \int_{x}^{+\infty} \frac{f(\xi)}{(x-\xi)^{1-\alpha}} d\xi. \tag{6}$$

For $\alpha = 1$, the representation (3) is not valid and has to be replaced by the formula

$$D_\theta^1 f(x) = [cos(\theta\pi/2) D_0^1 - sin(\theta\pi/2) D] f(x), \tag{7}$$

where the operator D_0^1 is related to the Hilbert transform as first noted by Feller in 1952 in his pioneering paper [21]

$$D_0^1 = \frac{1}{\pi} \frac{d}{dx} \int_{-\infty}^{+\infty} \frac{f(\xi)}{x-\xi} d\xi,$$

and D refers for the first standard derivative.

From the above relations one can see:

1- The quantum Riesz-Feller derivative is the Riesz-Feller derivative multiplied by -1.

2- The Riesz-Feller fractional derivative (in space) of order α and skewness θ can be expressed by the linear combination of the two-sided Riemann-Liouville differential operators.

3- When $\theta = 0$, the fractional Riesz-Feller derivative is changed to the Riesz derivative.

4- For c is any constant then $D_\theta^\alpha(c) = 0$.

In this paper, we consider the fractional Schrödinger equation with the quantum Riesz-Feller derivative that describes the wave function Ψ of a quantum particle that moves in a potential field with the potential V in the form:

$$i\hbar \frac{\partial \Psi(x,t)}{\partial t} = C_\alpha(m) D_\theta^\alpha \Psi(x,t) + V(x,t)\Psi(x,t), \quad t \ge 0, \quad x \in \mathbb{R}. \tag{8}$$

2.2 Non-Standard Discretization

The non-standard finite difference (NSFD) schemes were firstly proposed by Mickens [4], either for ordinary differential equations (ODEs) or partial differential equations (PDEs). A scheme is called non-standard if at least one of the following conditions is satisfied:

1- Nonlocal approximation is used.

2- Discretization of derivative is not traditional and use a nonnegative function i.e.,

when we want to approximate $\frac{dy}{dt}$ using Euler method we use $\frac{y(t+h)-y(t)}{\phi(h)}$ instead of $\frac{y(t+h)-y(t)}{h}$, where $\phi(h)$ is a continuous function of step size h, and the function $\phi(h)$ satisfies the following conditions:

$$\phi(h) = h + O(h^2), \;\; 0 < \phi(h) < 1, \;\; h \longrightarrow 0.$$

In addition to this replacement, if there are nonlinear terms in the differential equation, these are replaced by non-local approximation like for example

$$yx \longrightarrow \begin{cases} y_n x_{n+1}, \\ y_{n+1} x_n. \end{cases}$$

3 Discretization of the Cauchy-Type Problem for a Free Particle

In this section, we present the WA-NSFDM, to obtain the discretization of the fractional Schrödinger equation with the quantum Riesz-Feller derivative of order $\alpha,\; 1 < \alpha < 2$ for a free particle ($V = 0$) in the form

$$i\hbar \frac{\partial \Psi(x,t)}{\partial t} = C_\alpha(m) D_\theta^\alpha \Psi(x,t), \quad t > 0, \quad x \in \mathbb{R} \tag{9}$$

Existence and uniqueness theorems of the solution of Eq. (9) subject to an initial condition

$$\Psi(x,0)=f(x),\ \ x\in\mathbb{R},$$

and the boundary conditions

$$\Psi(x,t)\longrightarrow 0,\ as\ x\longrightarrow\pm\infty,$$

were introduced in [3] and the solution was given in terms of Fox H-function.

The problem of solving numerically equation (9) lies in a properly approximation of quantum Riesz-Feller derivative by a WA-NSFD scheme with a weight factor $\sigma\in[0,1]$.

Let us assume that the coordinates of the mesh points are

$$x_n=nh,\ n=...,-2,\ -1,\ 0,\ 1,\ 2,\ ...\ ,\quad t_m=m\triangle t,\ \ m=0,\ 1,\ 2,\ ...\ M\ ,$$

where $h=x_n-x_{n-1},\ \triangle t=t_m-t_{m-1}$. Let us define the approximation of the function $\Psi(x,t)$ on the grid (x_n,t_m) by $\Psi(x_n,t_m)=\Psi_n^m$. Eq. (9) can be written in the following form:

$$i\hbar\frac{\Psi_n^{m+1}-\Psi_n^m}{\varphi(\triangle t)}=C_\alpha(m)\frac{-h^{2-\alpha}}{(\phi(h))^2}\sum_{k=-\infty}^{+\infty}(\sigma\Psi_{n+k}^m+(1-\sigma)\Psi_{n+k}^{m+1})w_k+T_n^m, \tag{10}$$

where σ being the weight factor and the coefficients $w_k=w_k(\alpha,\theta)$ have the following form [14]:

$$w_k=\frac{-1}{2\Gamma(3-\alpha)}\times\begin{cases}[(|k|+2)^{2-\alpha}(2-\lambda)+(|k|+1)^{2-\alpha}(4\lambda-6) & \\ \quad +|k|^{2-\alpha}(6-6\lambda)+(|k|-1)^{2-\alpha}(4\lambda-2)+(|k|-2)^{2-\alpha}(-\lambda)]c_+ & \text{for } k\le -2,\\ (3^{2-\alpha}(2-\lambda)+2^{2-\alpha}(4\lambda-6)-6\lambda+6)c_++(2-\lambda)c_- & \text{for } k=-1,\\ (2^{2-\alpha}(2-\lambda)+4\lambda-6)(c_++c_-) & \text{for } k=0,\\ (3^{2-\alpha}(2-\lambda)+2^{2-\alpha}(4\lambda-6)-6\lambda+6)c_++(2-\lambda)c_+ & \text{for } k=1,\\ [(|k|+2)^{2-\alpha}(2-\lambda)+(|k|+1)^{2-\alpha}(4\lambda-6) & \\ \quad +|k|^{2-\alpha}(6-6\lambda)+(|k|-1)^{2-\alpha}(4\lambda-2)+(|k|-2)^{2-\alpha}(-\lambda)]c_- & \text{for } k\ge 2,\end{cases}$$

with

$$\lambda=\lambda(\alpha,\theta)=2-(\alpha+|\theta|).$$

The above replacements give rise to an error, the truncation error, denoted here by T_n^m. Its value will be discussed in Section 4.2. This technique has been used to simulate the fractional anomalous diffusion equation ([14], [22]), where $D_\theta^\alpha(\Psi)$ was approximated by the following formula:

$$\begin{aligned}D_\theta^\alpha(\Psi(x_n,t_m))\approx -\ &\Big[c_+\sum_{k=0}^{+\infty}\frac{1}{2(\phi(h))^2}[(2-\lambda)\Psi_{n-k+1}^m+(3\lambda-4)\Psi_{n-k}^m\\ &+(2-3\lambda)\Psi_{n-k-1}^m+\lambda\Psi_{n-k-2}^m]v_k+c_-\sum_{k=0}^{+\infty}\frac{1}{2(\phi(h))^2}[\lambda\Psi_{n+k+2}^m\\ &+(2-3\lambda)\Psi_{n+k+1}^m+(3\lambda-4)\Psi_{n+k}^m+(2-\lambda)\Psi_{n+k-1}^m]v_k\Big],\end{aligned} \tag{11}$$

with

$$\begin{aligned}v_k=\frac{1}{\Gamma(2-\alpha)}\int_{x_{n-k-1}}^{x_{n-k}}\frac{1}{(x_n-\xi)^{\alpha-1}}d\xi&=\frac{1}{\Gamma(2-\alpha)}\int_{x_{n+k}}^{x_{n+k+1}}\frac{1}{(\xi-x_n)^{\alpha-1}}d\xi\\ &=h^{2-\alpha}\frac{(k+1)^{2-\alpha}-k^{2-\alpha}}{\Gamma(3-\alpha)}.\end{aligned} \tag{12}$$

Neglecting the truncation error on scheme (10), one gets a computable difference scheme

$$i\hbar\frac{\Psi_n^{m+1}-\Psi_n^m}{\varphi(\triangle t)}=C_\alpha(m)\frac{-h^{2-\alpha}}{(\phi(h))^2}\sum_{k=-\infty}^{+\infty}(\sigma\Psi_{n+k}^m+(1-\sigma)\Psi_{n+k}^{m+1})w_k. \tag{13}$$

The proposed method is explicit for $\sigma = 1$, partially implicit for $0 < \sigma < 1$, especial case when $\sigma = 1/2$ then we have Crank-Nicholson scheme, and fully implicit for $\sigma = 0$ [23].

The numerical scheme (13), which included the unbounded domain $-\infty < x < +\infty$, has no practical implementations in computer simulations [14]. Here we solve this problem in the finite domain Ω: $L \le x \le R$ with boundary conditions for $t > 0$

$$\Psi(L,t) = \Psi(x_0,t) = g_L(t), \quad \Psi(R,t) = \Psi(x_N,t) = g_R(t). \tag{14}$$

We divide the domain Ω into N sub-domains with the step $h = (R-L)/N$. Here, we can observe additional points in the grid located outside the lower and upper limits of the domain Ω.
In order to introduce the Dirichlet boundary conditions, we propose a numerical treatment which assumes the same values of function Ψ outside the domain limits as the values predicted on boundary nodes x_0 and x_N.

$$\Psi(x_k,t) = \begin{cases} \Psi(x_0,t) \; for \; k < 0, \\ \Psi(x_N,t) \; for \; k > N. \end{cases}$$

Based on previous considerations we need to modify expressions (13) for the discretization of the quantum Riesz-Feller derivative. Thus we have

$$i\hbar \frac{\Psi_n^{m+1} - \Psi_n^m}{\varphi(\triangle t)} = C_\alpha(m) \frac{-h^{2-\alpha}}{(\phi(h))^2} \left[\sum_{k=-n}^{N-n} (\sigma \Psi_{n+k}^m + (1-\sigma)\Psi_{n+k}^{m+1}) w_k + (\Psi_0^m s_{L_n} + \Psi_N^m s_{R_{N-n}}) \right], \tag{15}$$

where

$$s_{L_n} = \sum_{k=-\infty}^{-n-1} w_k = c_- \cdot \frac{(n+2)^{2-\alpha}(2-\lambda) + (n+1)^{2-\alpha}(3\lambda-4) + n^{2-\alpha}(2-3\lambda) + (n-1)^{2-\alpha}}{2\Gamma(3-\alpha)}.$$

$$s_{R_n} = \sum_{k=n+1}^{\infty} w_k = c_+ \cdot \frac{(n+2)^{2-\alpha}(2-\lambda) + (n+1)^{2-\alpha}(3\lambda-4) + n^{2-\alpha}(2-3\lambda) + (n-1)^{2-\alpha}}{2\Gamma(3-\alpha)}.$$

Scheme (15) with the boundary condition (14) can be written after some simplification in the matrix form as:

$$\mathbf{C}\Psi^{\mathbf{m+1}} = \mathbf{A}\Psi^{\mathbf{m}} + \mathbf{B}, \tag{16}$$

where $\Psi^{\mathbf{m+1}}$ is the vector of unknown function values at time $m+1$, and

$$\mathbf{C} = \begin{pmatrix} 1 & 0 & 0 & 0 & \cdots & 0 & 0 \\ c_{-1} & 1+c_0 & c_1 & c_2 & \cdots & c_{N-2} & c_{N-1} \\ c_{-2} & c_{-1} & 1+c_0 & c_1 & \cdots & c_{N-3} & c_{N-2} \\ c_{-3} & c_{-2} & c_{-1} & 1+c_0 & \cdots & c_{N-4} & c_{N-3} \\ \vdots & \vdots & \vdots & \vdots & \ddots & \vdots & \vdots \\ c_{-N+1} & c_{-N+2} & c_{-N+3} & c_{-N+4} & \cdots & 1+c_0 & c_1 \\ 0 & 0 & 0 & 0 & \cdots & 0 & 1 \end{pmatrix},$$

$$\mathbf{A} = \begin{pmatrix} 1 & 0 & 0 & 0 & \cdots & 0 & 0 \\ a_{-1} & 1+a_0 & a_1 & a_2 & \cdots & a_{N-2} & a_{N-1} \\ a_{-2} & a_{-1} & 1+a_0 & a_1 & \cdots & a_{N-3} & a_{N-2} \\ a_{-3} & a_{-2} & a_{-1} & 1+a_0 & \cdots & a_{N-4} & a_{N-3} \\ \vdots & \vdots & \vdots & \vdots & \ddots & \vdots & \vdots \\ a_{-N+1} & a_{-N+2} & a_{-N+3} & a_{-N+4} & \cdots & 1+a_0 & a_1 \\ 0 & 0 & 0 & 0 & \cdots & 0 & 1 \end{pmatrix},$$

$$\mathbf{B} = [0,\ b_1,\ b_2, \ldots, b_{N-1}, 0]^T,$$

$$c_j = i\frac{C_\alpha(m)\varphi(\triangle t)h^{2-\alpha}}{\hbar(\phi(h))^2}(\sigma-1)w_j, \quad j = -N+1,\ ,\ldots,0\ ,\ \ldots,\ N-1,$$

$$a_j = i\frac{C_\alpha(m)\varphi(\triangle t)h^{2-\alpha}}{\hbar(\phi(h))^2}\sigma w_j, \quad j=-N+1,\ ,...,0\ ,\ ...,\ N-1,$$

$$b_n = i\frac{C_\alpha(m)\varphi(\triangle t)h^{2-\alpha}}{\hbar(\phi(h))^2}(\Psi_0^m s_{L_n} + \Psi_N^m s_{R_{N-n}}), \quad n=1,\ 2,\ ...,\ N-1.$$

4 Stability Analysis and Truncating Error

4.1 Stability Analysis

In this section, John von Neumann procedure is used to study the stability analysis of the weighted average scheme (15). Let us consider $\beta = -\frac{C_\alpha(m)\varphi(\triangle t)h^{2-\alpha}}{\hbar(\phi(h))^2}$, then scheme (15) can be written in the form

$$i(\Psi_n^{m+1} - \Psi_n^m) = \beta\left[\sum_{k=-n}^{N-n}(\sigma\Psi_{n+k}^m + (1-\sigma)\Psi_{n+k}^{m+1})w_k + (\Psi_0^m s_{L_n} + \Psi_N^m s_{R_{N-n}})\right]. \tag{17}$$

Theorem 1. The weighted average scheme (17) is conditionally stable.

Proof. Assuming that $\Psi_n^m = \xi^m e^{inhq}$ with q is the spatial wave number (which we assume to be purely real) [25] then Eq. (17) can be written in the following form

$$i(\xi^{m+1} - \xi^m)e^{inhq} = \beta\left[\sum_{k=-n}^{N-n}(\sigma\xi^m + (1-\sigma)\xi^{m+1})w_k e^{i(n+k)hq} + (s_{L_n} + s_{R_{N-n}}e^{iNhq})\xi^m\right],$$

dividing the last equation by $\xi^m e^{inhq}$ where $\frac{\xi^{m+1}}{\xi^m} = \eta \equiv \eta(q)$ is the amplification factor [24], we find:

$$i(\eta - 1) = \beta\left[\sum_{k=-n}^{N-n}(\sigma + (1-\sigma)\eta)w_k e^{ikhq} + (s_{L_n}e^{-inhq} + s_{R_{N-n}}e^{i(N-n)hq})\right],$$

so we can confirm that

$$\eta\left[i - \beta(1-\sigma)\sum_{k=-n}^{N-n} w_k e^{ikhq}\right] = i + \beta\left[\sigma\sum_{k=-n}^{N-n} w_k e^{ikhq} + z_n\right],$$

also

$$|\eta|.|i - \beta(1-\sigma)\sum_{k=-n}^{N-n} w_k e^{ikhq}| = |i + \beta\left[\sigma\sum_{k=-n}^{N-n} w_k e^{ikhq} + z_n\right]|,$$

where $z_n = s_{L_n}e^{-inhq} + s_{R_{N-n}}e^{i(N-n)hq}$ and $\overline{z_n}$ is the complex conjugate of z_n.

The scheme will be stable as long as $|\eta| \leq 1$, for all q i.e.,

$$|i + \beta(\sigma\sum_{k=-n}^{N-n} w_k e^{ikhq} + z_n)| \leq |i - \beta(1-\sigma)\sum_{k=-n}^{N-n} w_k e^{ikhq}|,$$

this inequality takes the next form depending on properties of the complex number norm:

$$\left[i + \beta(\sigma\sum_{k=-n}^{N-n} w_k e^{ikhq} + z_n)\right]\left[-i + \beta(\sigma\sum_{k=-n}^{N-n} w_k e^{-ikhq} + \overline{z_n})\right]$$
$$\leq \left[i - \beta(1-\sigma)\sum_{k=-n}^{N-n} w_k e^{ikhq}\right]\left[-i - \beta(1-\sigma)\sum_{k=-n}^{N-n} w_k e^{-ikhq}\right].$$

The above inequality can be written as:

$$\beta\sigma^2\sum_{k=-n}^{N-n} w_k e^{ikhq}\sum_{k=-n}^{N-n} w_k e^{-ikhq}+\beta\sigma(\overline{z_n}\sum_{k=-n}^{N-n} w_k e^{-ikhq}+z_n\sum_{k=-n}^{N-n} w_k e^{ikhq})$$

$$+\beta z_n\overline{z_n}-i\sigma(\sum_{k=-n}^{N-n} w_k e^{ikhq}-\sum_{k=-n}^{N-n} w_k e^{-ikhq})-i(z_n-\overline{z_n})$$

$$\leq i(1-\sigma)(\sum_{k=-n}^{N-n} w_k e^{ikhq}-\sum_{k=-n}^{N-n} w_k e^{-ikhq})+\beta(1-\sigma)^2\sum_{k=-n}^{N-n} w_k e^{ikhq}\sum_{k=-n}^{N-n} w_k e^{-ikhq}. \quad (18)$$

Let $z_n=r_n e^{i\theta_n}$, then the previous inequality (18) after some simplification:

$$\beta\sigma r_n(e^{-i\theta_n}\sum_{k=-n}^{N-n} w_k e^{ikhq}+e^{i\theta_n}\sum_{k=-n}^{N-n} w_k e^{-ikhq})+\beta r_n^2-2sin\theta_n$$

$$\leq i(\sum_{k=-n}^{N-n} w_k e^{ikhq}-\sum_{k=-n}^{N-n} w_k e^{-ikhq})+\beta(1-2\sigma)\sum_{k=-n}^{N-n} w_k e^{ikhq}\sum_{k=-n}^{N-n} w_k e^{-ikhq},$$

which equivalent to

$$\beta[\sigma r_n.2\sum_{k=-n}^{N-n} w_k cos(\theta_n-khq)-(1-2\sigma)(\sum_{k=-n}^{N-n} w_k^2+2\sum_{k=-n,v=-n,k\neq v}^{N-n} w_k w_v cos(k-v)hq)+r_n^2]$$

$$\leq 2sin\theta_n-2\sum_{k=-n}^{N-n} w_k sin(khq).$$

So the scheme (17) is stable under the condition:

$$\beta B-A\leq 0, \quad (19)$$

with

$$A=2sin\theta_n-2\sum_{k=-n}^{N-n} w_k sin(khq),$$

$$B=2\sigma r_n\sum_{k=-n}^{N-n} w_k cos(\theta_n-khq)-(1-2\sigma)(\sum_{k=-n}^{N-n} w_k^2+2\sum_{k=-n,v=-n,k\neq v}^{N-n} w_k w_v cos(k-v)hq)+r_n^2.$$

4.2 Truncating Error

Theorem 2. The truncating error of WA-NSFD scheme (10) is:

$$T_n^m=O(\varphi(\triangle t)+\phi(h)+h^{2-\alpha}).$$

Proof. From the definition of truncating error given by Eq. (10), one gets

$$T_n^m=i\hbar\frac{\Psi_n^{m+1}-\Psi_n^m}{\varphi(\triangle t)}+C_\alpha(m)\frac{h^{2-\alpha}}{(\phi(h))^2}\sum_{k=-\infty}^{+\infty}(\sigma\Psi_{n+k}^m+(1-\sigma)\Psi_{n+k}^{m+1})w_k, \quad (20)$$

depending on Taylor series expansion we find (for all n)

$$\frac{\Psi_n^{m+1}-\Psi_n^m}{\varphi(\triangle t)}=\Psi_t+\frac{1}{2}\cdot\Psi_{tt}\cdot(\varphi(\triangle t))+\frac{1}{6}\Psi_{ttt}\cdot(\varphi(\triangle t))^2+..., \quad (21)$$

and Eq.(11) takes the form (for all m)

$$D_{\theta}^{\alpha}(\Psi_n^m) \approx - \Bigg[c_+ \sum_{k=0}^{+\infty} [\Psi_{xx} + \frac{1}{2}\phi(h)\Psi_{xxx} + \frac{1}{48}(4+12\lambda)(\phi(h))^2\Psi_{xxxx} + ...]v_k + c_- \sum_{k=0}^{+\infty} [\Psi_{xx} + \frac{1}{2}\phi(h)\Psi_{xxx} + \frac{1}{48}(4+12\lambda)(\phi(h))^2\Psi_{xxxx} + ...]v_k \Bigg]. \tag{22}$$

We mention here (for example) the Taylor expansion for Ψ_{n-k+1}^m which we have used to write Eq. (11) in the form (22)

$$\Psi_{n-k+1} = \Psi_{n-k} + \Psi_x \cdot \phi(h) + \frac{1}{2}\Psi_{xx} \cdot (\phi(h))^2 + \frac{1}{6}\Psi_{xxx} \cdot (\phi(h))^3 + \frac{1}{24}\Psi_{xxxx} \cdot (\phi(h))^4 + \dots .$$

Eq. (22) can be written, using Eq. (12), in the following form

$$D_{\theta}^{\alpha}(\Psi_n^m) \approx \frac{h^{2-\alpha}}{(\phi(h))^2} \sum_{k=-\infty}^{+\infty} (\Psi_{n+k}^m) w_k = -(c_+ + c_-)[\Psi_{xx} + \frac{1}{2}\phi(h)\Psi_{xxx} + \frac{1}{48}(4+12\lambda)(\phi(h))^2\Psi_{xxxx} + ...] \sum_{k=0}^{+\infty} h^{2-\alpha} \frac{(k+1)^{2-\alpha} - k^{2-\alpha}}{\Gamma(3-\alpha)}. \tag{23}$$

Inserting these expressions (21, 23) into Eq. (20), the local truncation error is

$$T_n^m = O(\varphi(\triangle t) + \phi(h) + h^{2-\alpha}).$$

Accordingly, our scheme is convergent under the condition (19).

5 Numerical Examples

In this section we present the results obtained by the present numerical approach (16) with $\varphi(\triangle t) = sinh(\triangle t)$, $\phi(h) = sinh(h)$.

Example 1. Consider the space fractional Schrödinger equation with the quantum Riesz-Feller derivative

$$\frac{\partial \Psi(x,t)}{\partial t} = -iD_{\theta}^{\alpha}\Psi(x,t), \quad -2 < x < 2, \quad t > 0, \quad 1 < \alpha < 2, \tag{24}$$

with the initial condition:

$$\Psi(x,0) = 1 + cosh(2x),$$

the boundary conditions:

$$\Psi(-2,t) = 1 + cosh(-4)e^{-4it}, \quad \Psi(2,t) = 1 + cosh(4)e^{-4it},$$

and the exact solution when $\alpha = 2$ [8] is:

$$\Psi(x,t) = 1 + cosh(2x)e^{-4it}, \quad -2 \le x \le 2.$$

Table(1) shows the maximum error between the norm of the numerical solution obtained by using the WA-NSFDM and the norm of the exact solution, is smaller than the maximum error between the norm of the numerical solution obtained by using the FDM and the norm of the exact solution, when $\sigma = 1$ at $t = 1$, using $N = 10$ and different values of M.

Table(2) shows the maximum errors between the norm of the numerical solution obtained by using the WA-NSFDM and the norm of the exact solution, when $\sigma = 1,\ 0.5,\ 0$, at $t = 1$, using $N = 50$ and different values of M also it shows the stability bound (SB) (19).

The behavior of the real parts of the analytical and numerical solutions by means of the WA-NFDM ($\sigma = 1$) with different values of α and θ when $0 < t \le 0.6$ are presented in Figures (1) and (2).

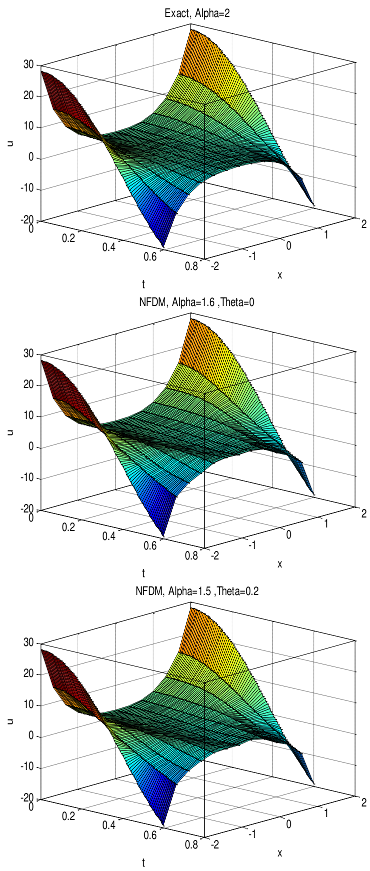

Fig. 1: Solution of the real part of example (1) for different values of α, θ and $N = 12,\ M = 100$.

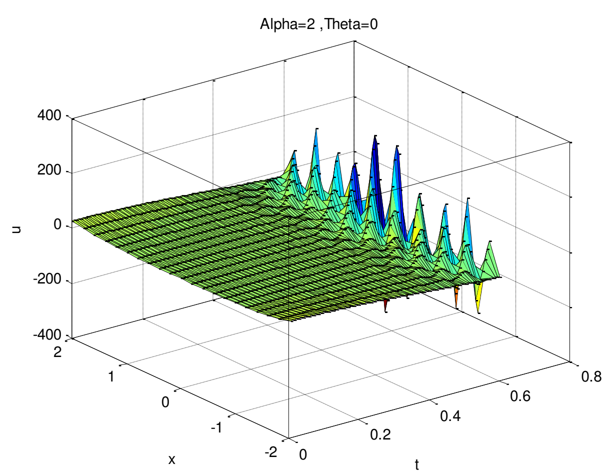

Fig. 2: Unstable solution of the real part of example (1) when $N = 20,\ M = 100,\ \alpha = 2,\ \theta = 0$, here $SB = 0.0151$.

Table 1: The maximum error for example (1) when $\alpha = 2$ and $N = 10$ at t=1 using WA-NSFDM and FDM ($\sigma = 1$).

M	max-error-WA-NSFD	max-error-SFD
100	1.2072e-01	3.9669e-01
500	1.7256e-02	3.9339e-01
1000	8.5100e-03	3.9404e-01
5000	1.6870e-03	3.9449e-01
10000	8.4269e-04	3.9455e-01

Table 2: The maximum error for example (1) when $\alpha = 2$ and $N = 50$ at t=1 using WA-NSFDM with $\sigma = 1,\ 0.5,\ 0$ and the (SB)

	$(\sigma = 1)$		$(\sigma = 0.5)$		$(\sigma = 0)$	
M	max-error	SB	max-error	SB	max-error	SB
50	divergent	9.6e-04	6.2345e-01	-9.8e-04	2.7353e-01	-9.6e-04
200	divergent	9.8e-04	1.5703e-01	-9.8e-04	1.2620e-01	-9.8e-04
500	divergent	9.8e-04	4.2314e-02	-9.8e-04	6.3040e-02	-9.8e-04
1000	divergent	9.8e-04	2.3245e-02	-9.8e-04	3.3042e-02	-9.8e-04
2000	divergent	9.8e-04	1.8051e-03	-9.8e-04	1.9655e-03	-9.8e-04

Example 2. Consider the space fractional Schrödinger equation with the quantum Riesz-Feller derivative

$$\frac{\partial \Psi(x,t)}{\partial t} = -iD_{\theta}^{\alpha}\Psi(x,t), \quad -2 < x < 2, \ \ t > 0, \ \ 1 < \alpha < 2, \tag{25}$$

with the initial condition:

$$\Psi(x,0) = e^{3ix},$$

the boundary conditions:

$$\Psi(-2,t) = e^{3i(-2+3t)}, \qquad \Psi(2,t) = e^{3i(2+3t)},$$

and the exact solution when $\alpha = 2$ is given as follows [8]:

$$\Psi(x,t) = e^{3i(x+3t)}, \quad -2 \le x \le 2.$$

Table(3) shows the maximum errors of WA-NSFDM, when $\sigma = 1,\ 0.5,\ 0$, between norm of the exact solution and norm of the numerical solutions at $t = 1$, using $M = 1000$ and different values of N also it shows the (SB) (19).

Table(4) shows the maximum errors of WA-NSFDM, when $\sigma = 1,\ 0.5,\ 0$, between norm of the exact solution and norm of the numerical solutions at $t = 1$, using $N = 40$ and different values of M also it shows the (SB) (19).

The behavior of the imaginary parts of the analytical and numerical solution by means of the WA-NFDM ($\sigma = 1$) with different values of α and θ when $0 < t \le 0.6$ are presented in Figures (3) and (4).

Table 3: The max-error for example (2) when $\alpha = 2$ and $M = 1000$ at t=1 using WA-NSFDM with $\sigma = 1,\ 0.5,\ 0$ and the (SB) with different value of N.

	$(\sigma = 1)$		$(\sigma = 0.5)$		$(\sigma = 0)$	
N	max-error	SB	max-error	SB	max-error	SB
20	2.9664e-01	-1.5e-02	2.8405e-01	-1.5e-02	2.9954e-01	-1.5e-02
50	divergent	9.8e-04	4.3375e-02	-9.8e-04	7.1492e-02	-9.8e-04
100	divergent	1.2e-04	1.1069e-02	-1.2e-04	4.8963e-02	-1.2e-04
200	divergent	1.5e-05	7.7360e-03	-1.5e-05	4.7809e-02	-1.5e-05

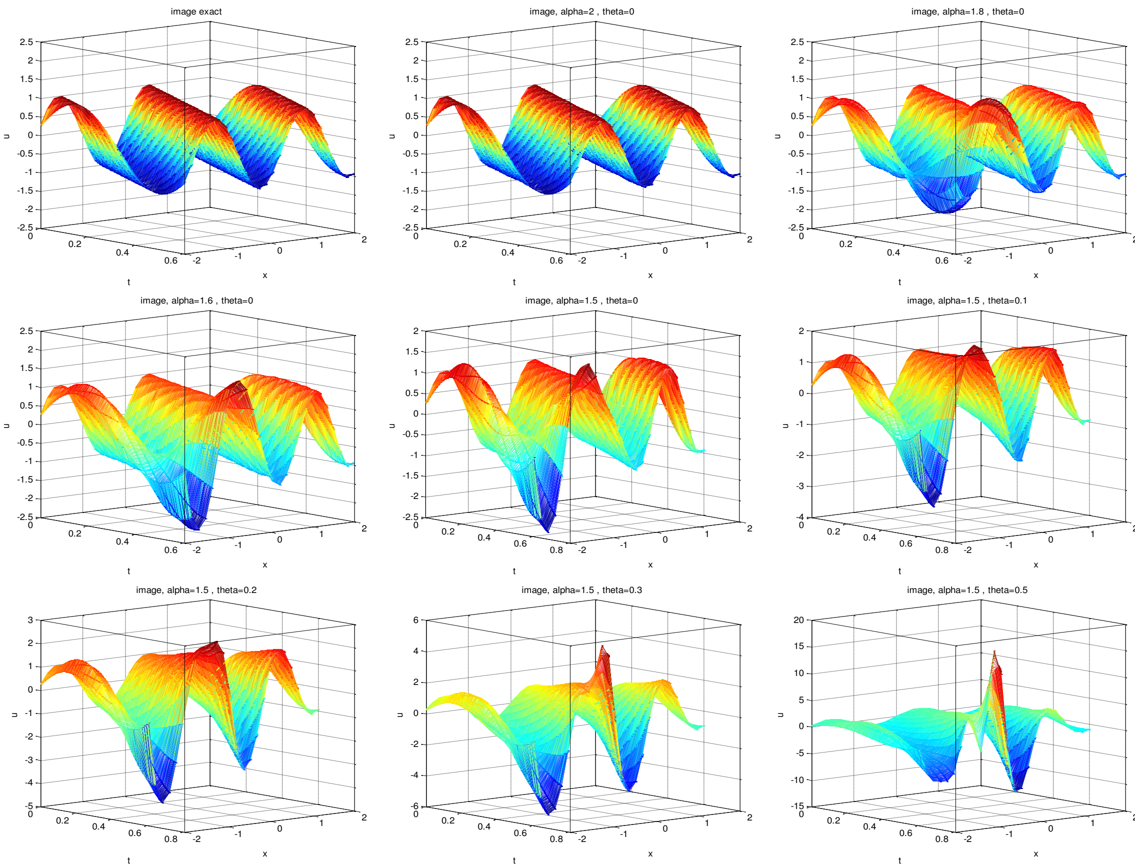

Fig. 3: Behavior of the imaginary part of solution of example (2) for different values of α, θ and $N = 12,\ M = 100$.

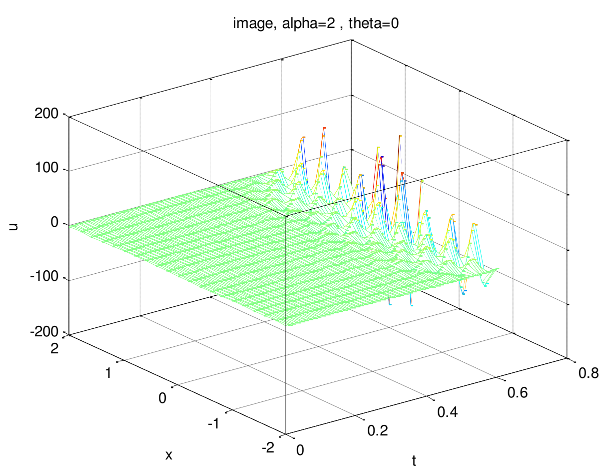

Fig. 4: Unstable solution of the imaginary part of example (2) when $N = 20,\ M = 100,\ \alpha = 2,\ \theta = 0$, here $SB = 1.5128e-02$.

Table 4: The max-error for example (2) when $\alpha = 2$ and $N = 40$ at t=1 using WA-NSFDM with $\sigma = 1,\ 0.5,\ 0$ and the (SB) with different value of M.

M	$(\sigma = 1)$ max-error	SB	$(\sigma = 0.5)$ max-error	SB	$(\sigma = 0)$ max-error	SB
10	divergent	1.5e-03	6.5126e-01	-1.9e-03	8.8342e-01	-1.5e-03
100	divergent	1.8e-03	6.9029e-02	-1.9e-03	4.2900e-01	-1.8e-03
200	divergent	1.9e-03	3.3151e-02	-1.9e-03	2.2612e-01	-1.9e-03
500	divergent	1.9e-03	2.6544e-02	-1.9e-03	2.6544e-02	-1.9e-03

Example 3. Consider the space fractional Schrödinger equation with the quantum Riesz-Feller derivative

$$\frac{\partial \Psi(x,t)}{\partial t} = -iD_{\theta}^{\alpha}\Psi(x,t) - iv(x,t)\Psi(x,t),\ \ 0 < x < 2\pi,\ \ t > 0,\ \ 1 < \alpha < 2, \tag{26}$$

such that

$$v(x,t) = 3/2 + sin\frac{\theta\pi}{2} + cos\frac{\theta\pi}{2},$$

with the initial condition:

$$\Psi(x,0) = sin(x),$$

the boundary conditions:

$$\Psi(0,t) = 0, \quad \Psi(2,t) = sin(2)e^{(-3it/2)},$$

and the exact solution is:

$$\Psi(x,t) = sin(x)e^{(-3it/2)},\ \ 0 \le x \le 2\pi.$$

Table(5) shows the maximum errors of WA-NSFDM, when $\sigma = 1,\ 0.5,\ 0$, between norm of the exact solution and norm of the numerical solutions, using $N = 10,\ M = 100,\ \theta = 0$ and different values of α when $t = 0.1$ also it shows the (SB) (19).

Table(6) shows the maximum errors of WA-NSFDM, when $\sigma = 1,\ 0.5,\ 0$, between norm of the exact solution and norm of the numerical solutions, using $N = 10,\ M = 100,\ \alpha = 1.7$ and different values of θ when $t = 0.1$ also it shows the (SB) (19).

Figs. (5) show the behavior of the real part of the exact solution and the solutions of example (3) using the WA-NSFDM $(\sigma = 1)$ for different values of α and θ when $N = 15,\ M = 10$.

Figs. (6) show the behavior of the real part of the solutions of example (3) using the WA-NSFDM $(\sigma = 1)$ for $\alpha = 2$ and $\theta = 0$ when $N = 10,\ M = 10$.

Table 5: The max-error for example (3) when $N = 10,\ M = 100,\ \theta = 0$ and different values of α, using WA-NSFD with $\sigma = 1,\ 0.5,\ 0$ and the (SB).

α	$(\sigma = 1)$ max-error	SB	$(\sigma = 0.5)$ max-error	SB	$(\sigma = 0)$ max-error	SB
2	divergent	7.5e-03	1.0960e-02	-7.5e-03	1.1075e-02	-7.5e-03
1.7	divergent	6.8e-02	1.0873e-02	-6.8e-02	1.0096e-02	-6.8e-02
1.4	divergent	1.2e-01	8.1281e-03	-1.2e-01	8.0639e-03	-1.2e-01
1.1	divergent	1.8e-01	5.7612e-03	-1.8e-01	5.6717e-03	-1.8e-01
1	divergent	1.9e-01	7.6605e-04	-1.9e-01	2.4310e-04	-1.9e-01

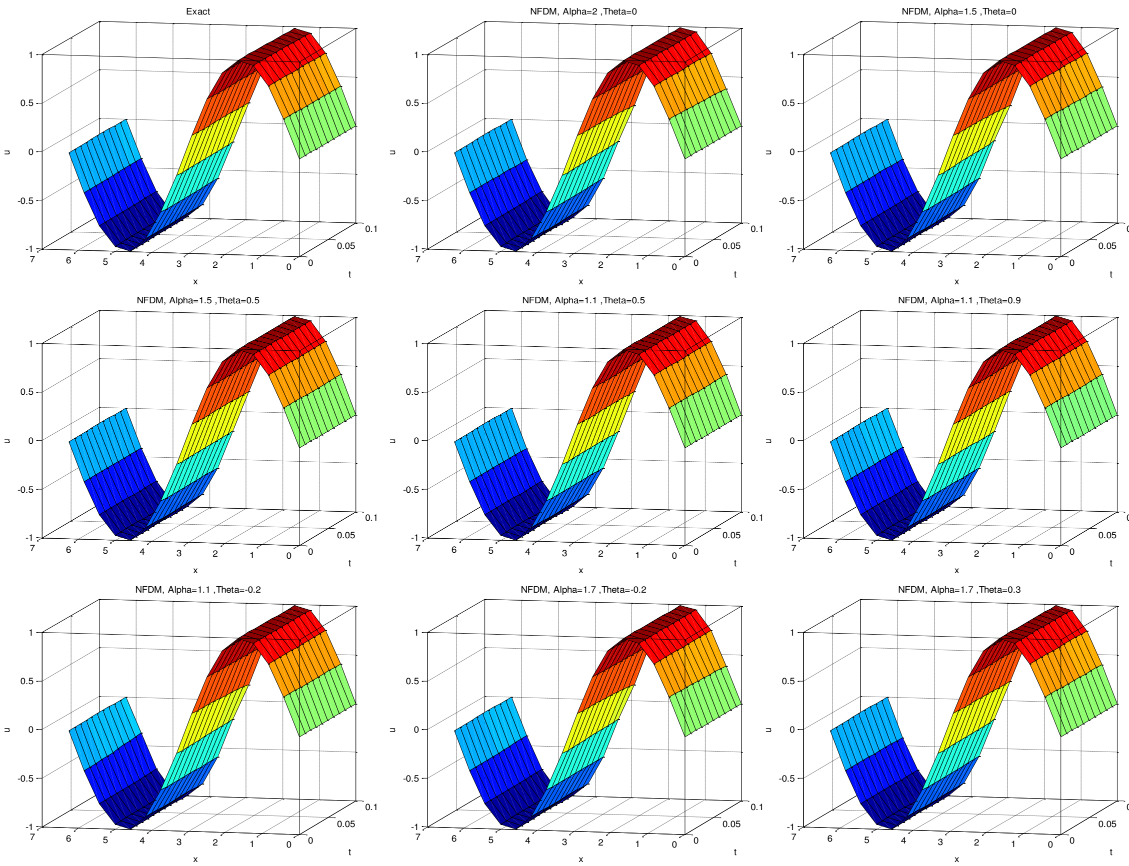

Fig. 5: Behavior of the real part solutions of example (3) for different values of α and θ and $N = 15,\ M = 10$.

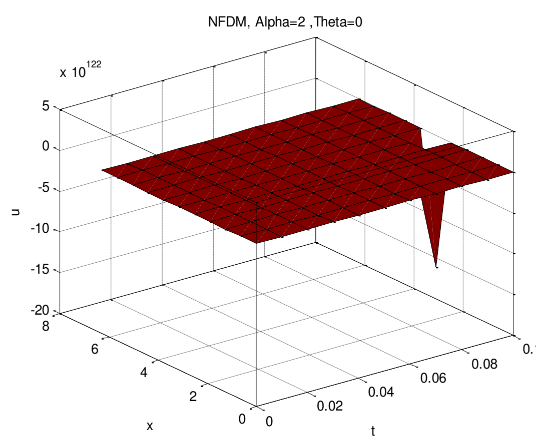

Fig. 6: Unstable solution of the real part of example (3) when $N = 10,\ M = 10,\ \alpha = 2,\ \theta = 0$, here $SB = 7.5382e-03$.

Table 6: The max-error for example (3) when $N = 10,\ M = 100,\ \alpha = 1.7$ and different values of θ, using WA-NSFD with $\sigma = 1,\ 0.5,\ 0$ and the (SB).

	$(\sigma = 1)$		$(\sigma = 0.5)$		$(\sigma = 0)$	
θ	max-error	SB	max-error	SB	max-error	SB
0	divergent	6.8e-02	1.0132e-02	-6.8e-02	1.0096e-02	-6.8e-02
0.1	divergent	6.2e-02	8.4556e-03	-6.2e-02	8.4522e-03	-6.2e-02
0.2	divergent	4.8e-02	6.8251e-03	-4.8e-02	6.9052e-03	-4.8e-02
0.3	divergent	2.8e-02	6.0464e-03	-2.8e-02	6.1157e-03	-2.8e-02
-0.2	divergent	5.6e-02	1.4159e-02	-5.6e-02	1.3923e-02	-5.6e-02

6 Conclusions

In this paper, we used WA-NSFDM to introduce numerically the approximate solution of a fractional Schrödinger equation with the quantum Riesz-Feller derivative. The proposed method is based on choosing the weight factor σ. The main advantage of this method is, it can be explicit or implicit with large stability regions as we see in tables (2-6). Special attention is given to study the stability and consistency of proposed methods. To execute this aim we have resorted to the kind of John Von Neumann stability analysis. Some numerical results are used to show the accuracy of the WA-NSFDM and some figures are used to demonstrate how the solutions change when α and θ take different values. All computations in this paper are performed using MATLAB programming.

Acknowledgment

The authors wish to thank the referees for their constructive comments and suggestions which improved the present paper.

References

[1] N. Laskin, Fractional Schrödinger equation, University of Toronto, 1-18, 2002.

[2] R. Becerril, F.S. Guzman, A. Rendon-Romero and S. Valdez-Alvarado, Solving the time-dependent Schrödinger equation using finite difference methods, *Rev. Mex. Fis.* **54**(2), 120-132 (2008).

[3] B. Al-Saqabi, L. Boyadjiev and Yu. Luchko, Comments on employing the Riesz-Feller derivative in the Schrödinger equation, *Eur. Phys. J. Spec. Topic.* **222**, 1779-1794 (2013).

[4] R. E. Mickens, Application of nonstandard finite difference schemes, World Scientific Publishing Co. Pte. Ltd., 2000.

[5] N. H. Sweilam and T. A. Assiri, Numerical simulations for the space-time variable order nonlinear fractional wave equation, *J. Appl. Math.* Article ID 586870, **2013**, 7 pages (2013).

[6] N. H. Sweilam and T. A. Assiri, Non-standard Crank-Nicholson method for solving the variable order fractional cable equation, *Appl. Math. Inf. Sci.* **2**, 943-951 (2015).

[7] N. H. Sweilam and T. F. Almajbri, Large Stability Regions method for the two-dimensional fractional diffusion equation, *Progr. Fract. Differ. Appl.* **1**(2), 123-131 (2015).

[8] A. Bibi, A. Kamran, U. Hayat and S. Mohyud-Din, New iterative method for time-fractional Schrödinger equations,*World J. Mod. Simul.* **9**(2), 89–95 (2013).

[9] L. Wei, Y. He, X. Zhang and S. Wang, Analysis of an implicit fully discrete local discontinous Galerkin methods fort he time-fractional Schrödinger equation, *Finite Elem. Anal. Des.* **59**, 28-34 (2012).

[10] A. Mohebbi, M. Abbaszadeh and M. Dehghan, The use of a meshless technique based on collocation and radial basis functions for solving the time fractional nonlinear Schrödinger equation arising in quantum mechanics, *Eng. Anal. Bound. Elem.* **37**, 475–485 (2013).

[11] A. H. Bhrawy, E. H. Doha, S. S. Ezz-Eldien and R. A. Van Gorder, A new Jacobi spectral collocation method for solving 1 + 1 fractional Schrodinger equations and fractional coupled Schrödinger systems, *Eur. Phys. J. Plus* **129**, 260 (2014).

[12] A. H. Bhrawy and M. A. Abdelkawy, A fully spectral collocation approximation for multi-dimensional fractional Schrödinger equations, *J. Comput. Phys.* **294**, 462-483 (2015).

[13] F. Mainardi, Y. Luchko and G. Pagnini, The fundamental solution of the space-time fractional diffusion equation, *Fract. Calc. Appl. Anal.* **4**(2), 153–192 (2001).

[14] M. Ciesielski and J. Leszczynski, Numerical solutions to boundary value problem for anomalous diffusion equation with Riesz-Feller fractional operator, *J. Theor. Appl. Mech.* **44**(2) 393-403 (2006).

[15] N. H. Sweilam and T. A. Assiri, Error analysis of explicit finite difference approximation for the space fractional wave equations, *SQU J. Sci.* **17**, 245-253 (2012).

[16] R. Herrmann, Fractional Calculus, An introduction for physicists, World Scientific Publishing Co. Pte. Ltd., 2011.
[17] F. Silva, J. A. P. F. Marào, J. C. Alves Soares and E. Capelas de Oliveira, Similarity solution to fractional nonlinear space-time diffusion-wave equation, *J. Math. Phys.* **56**, 1-16 (2015).
[18] I. Podlubny, Fractional differential equations, Academic Press, San Diego, 1999.
[19] H. J. Haubold, A. M. Mathai and R. K. Saxena, Solutions of fractional reaction-diffusion equations in terms of the H-function, http://arxiv.org/abs/0704.0329v2 (2007).
[20] G. H. Zheng and T. Wei, Two regularization methods for solving a Riesz-Feller space-fractional backward diffusion problem, *Inverse Probl.* **26**, 1-22 (2010).
[21] W. Feller, On a generalization of Marcel Riesz' potentials and the semi-groups generated by them, Meddelanden Lunds Universitets Matematiska Seminarium (Comm. Sém. Mathém. Université de Lund), Tome suppl. dédié à M. Riesz, Lund, 73, (1952).
[22] M. Ciesielski and J. Leszczynski, Numerical treatment of an initial-boundary value problem for fractional partial differential equations, *Signal Proc.* **86**(10), 2503-3094 (2006).
[23] S. B. Yuste, Weighted average finite difference methods for fractional diffusion equations, *J. Comput. Phys.* **216**, 264-274 (2006).
[24] K. W. Morton and D. F. Mayers, Numerical solution of partial differential equations, Cambridge University Press, Cambridge, 1994.
[25] S. B. Yuste and L. Acedo, On an explicit finite difference method for fractional diffusion equations. Preprint at http://arxiv.org/abs/cs.NA/0311011, (2003).